Available online at www.sciencedirect.com
ScienceDirect
Surface & Coatings Technology 202 (2008) 2162–2168
SURFACE & COATINGS TECHNOLOGY
www.elsevier.com/locate/surfcoat

Electron beam deposited VC and NbC thin films on titanium: Hardness and energy-dispersive X-ray diffraction study

D. Ferro [a], J.V. Rau [a], A. Generosi [b], V. Rossi Albertini [b], A. Latini [c], S.M. Barinov [d,*]

[a] *Istituto per lo Studio dei Materiali Nanostrutturati, CNR, Piazzale Aldo Moro 5-00185 Rome, Italy*
[b] *Istituto di Struttura della Materia, CNR, via del Fosso del Cavaliere, 100-00133 Rome, Italy*
[c] *Universitá di Roma La Sapienza, Dipartimento di Chimica, Piazzale Aldo Moro 5-00185 Rome, Italy*
[d] *Institute for Physical Chemistry of Ceramics, Russian Academy of Sciences, Ozernaya 48, Moscow, 119361, Russia*

Received 28 June 2007; accepted in revised form 5 September 2007
Available online 18 September 2007

Abstract

Films of VC and NbC of about 200 nm thickness were electron beam deposited on the sandblasted surface of metallic Ti substrates, preheated at 350 and 500 °C, to improve the surface hardness of Ti implants intended for application in orthopaedics. According to both standard angular-dispersive X-ray diffraction measurements and rocking curve analysis performed by energy-dispersive X-ray diffraction, the films were found to be textured preferentially along the (200) crystallographic direction. The (200)-oriented crystallites are randomly rotated around their growth axes, with no correlation among adjacent domains. The measured intrinsic hardness of the films is 24–25 GPa for VC and 18–21 GPa for NbC.

Keywords: Thin films; Carbides; Electron beam deposition; Hardness; X-ray diffraction

1. Introduction

Carbides of transition metals of groups IV and V have high melting points, good mechanical properties, such as hardness, and excellent resistance to chemical attacks [1–3]. Due to these properties, coatings composed of such materials are well suited to be used in surface engineering of mechanical components, tools, turbine blades, *etc.* [4]. The carbon diffusing from the coating into the substrate can provide a metallurgically bonded carbide coating at the substrate surface [5]. The surface engineering of titanium and titanium-based alloys seems to be of special interest due to their widespread clinical use as implant materials providing a good combination of mechanical properties and biocompatibility [6]. Clinical problems sometimes encountered with titanium implants and their abutments are related to the relative softness of these materials, which results in possible damages [6], and in a poor resistance against oxidation in the harsh conditions of the body fluids [7]. Transient titanium oxides forming on the titanium surface reduce the wear resistance. A high wear rate may result in wear debris accumulation, adverse cellular response and implant loosening. The addition of a thin hard coating to the surface of titanium might overcome those problems, thus protecting titanium against oxidation and improving surface hardness. Continuous research has been directed towards surface modification of titanium and, to date, numerous coating techniques are available to deposit carbide coatings with improved properties and wear characteristics [8]. Each coating process has inherent advantages and disadvantages that affect the microstructure and, as a consequence, the properties of coatings [8]. Thin titanium carbide films deposited on titanium substrates by pulsed laser ablation (PLAD) demonstrated to possess an excellent bioactivity towards osseointegration [9]. Electron beam deposited (EBD) TiC coatings showed to increase the surface hardness of titanium effectively [10].

Alternatively to TiC, other bio-inactive refractory hard transient metals carbides of NaCl-type structure may be deposited on a titanium surface. In particular, niobium carbide coatings were shown to decrease the wear rate of metals significantly [11]. The EBD technique has successfully been employed to deposit thin ZrC and HfC [12], as well as TaC [13]

* Corresponding author. Tel.: +7 495 4379892; fax: +7 495 4379893.
E-mail address: barinov_s@mail.ru (S.M. Barinov).

0257-8972/$ - see front matter © 2007 Elsevier B.V. All rights reserved.
doi:10.1016/j.surfcoat.2007.09.008

films on titanium, the Vickers hardness of the films being as high as 26, 19 and 12.4 GPa for ZrC, HfC and TaC, respectively.

The present work is aimed to deepen the study of the EB deposited refractory carbide coatings, VC and NbC, on titanium. The deposition was performed at two different substrate preheating temperatures (350 and 500 °C), the intrinsic hardness of the films was evaluated, and the structure of the films was investigated both using the conventional (angular-dispersive) X-ray diffraction technique and its energy-dispersive counterpart [14,15].

2. Experimental

The targets for EBD were fabricated using initial carbide powders (98% pure; Aldrich Chemical Co.) that were hot pressed into 18 mm diameter and 5 mm height cylindrical pellets. The pellets were placed into a refractory crucible and, then, inserted into a water-cooled electron beam gun (EVI-8, Ferrotec). The gun is equipped with a magnetic lenses system that allows a 270° deflection of the beam for avoiding contamination of the evaporating material with the tungsten of the emitting filament. The substrate was heated under vacuum at 5×10^{-3} Pa in a chamber containing a high-power halogen lamp. The deposition process was performed at an accelerating voltage of −3.5 kV and at an emission current ranging from 130 to 200 mA. The electron beam pattern was set circular, to ensure uniform consumption of the evaporating target. The deposition was performed for several minutes at the substrate preheating temperatures of 350 and 500 °C, the temperature being measured by a thermocouple (±10 °C error). The thermocouple was positioned on the top of the substrate. No significant spitting of the target was observed. Before the deposition, the titanium substrate was sandblasted with a 60-grid SiC abrasive powder to provide a surface roughness R_a, of approximately 1.6×10^{-6} m, necessary to guarantee the best cell adhesion of the implanted device to the substrate surface.

The thickness of the growing films as well as the deposition rates were real-time monitored by a quartz microbalance. The microbalance is based on the acoustic impedance of the deposited material, that is the product between the acoustic velocity of sound in the material and the material density. For a given material, the acoustic velocity of sound is given by the formula:

$$V=\sqrt{\frac{\mathrm{BM}}{\rho}} \tag{1}$$

where BM is the bulk modulus of elasticity of the material and ρ is the density. The microbalance controller needs to be calibrated by measuring the so-called "z factor", which is given by the ratio between the acoustic impedance of quartz and the acoustic impedance of the material to deposit. The thicknesses of the deposited VC and NbC films estimated by the microbalance resulted to be 0.2 μm.

Preliminarily, scanning electron microscopy (SEM) of the samples images were taken by a LEO 1450 VP microscope coupled with an X-ray energy-dispersive system (EDS) INCA. Then, conventional X-ray diffraction (XRD) measurements were performed by a Philips X'Pert PRO apparatus (Cu $K_{\alpha1}$ radiation, $\lambda=1.54056$ Å, graphite monochromator, JCPDS cards # 73-0476 (VC), # 38-1362 (NbC), and # 88-2321 (Ti)) for a gross structural characterization of the films.

Finally, the fine details of the films structure were studied by means of the energy-dispersive X-ray diffraction (EDXD), whose general principles have been fully described elsewhere [14,15]. The main feature of this technique is the use of an X-ray "white beam" (the photons have various energies) to collect the diffraction pattern keeping the scattering angle fixed, while in the conventional XRD method, the photons are monochromatic and the scattering angle is varied. The EDXD method allows not only to identify the phase composition but also to easily collect the rocking curve (RC) of each diffracted peak with reduced acquisition times and high accuracy [15]. The rocking curve of a polycrystalline sample represents the statistical distribution of the crystallites orientation around the mean growth axes, *i.e.* the degree epitaxy of the material. The rocking curve is the plot of a peak intensity as a function of the angle alpha between the scattering vector and the normal to the surface coating, as shown in Fig. 1. Moreover, when RC measurements are performed, the energy-dispersive mode is particularly efficient, since all the Bragg peaks in the selected q-region are collected simultaneously. This allows the acquisition of the RC of all the visible reflections, providing a more accurate information on the sample texture. The ED diffractometer is a non-commercial apparatus [14], equipped with two arms pivoting around the optical centre of the instrument, where the sample holder is located. A white X-ray radiation is produced by a W-anode X-ray tube (12–55 keV) and is collimated upstream and downhill the sample by four W slits. The detection is accomplished by an EG&G high purity germanium solid state detector connected to a PC *via* ADCAM hardware. The signal is amplified, analogue to digital converted and finally processed by a home made software, which provides the diffraction patterns plots. Neither monochromator nor goniometer is required in the energy-dispersive mode.

The hardness of the composite film/substrate system was measured with a Leica VMHT apparatus equipped with a standard Vickers pyramidal indenter. The loading and unloading speed was 5×10^{-6} m/s, time under the peak load being 15 s. Indentations were made with 5 loads ranging from 0.098 to 19.6 N. To separate the hardness, H_c, of the film/substrate system on its constituents from the film (H_f) and the substrate (H_s), a Jönsson and Hogmark model based on an area law-of-mixture approach was used [16]. Further, the indentation size

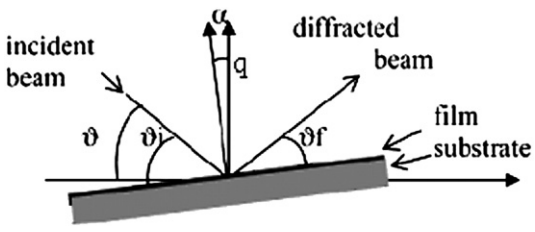

Fig. 1. Scheme of the geometric setup during a rocking curve analysis.

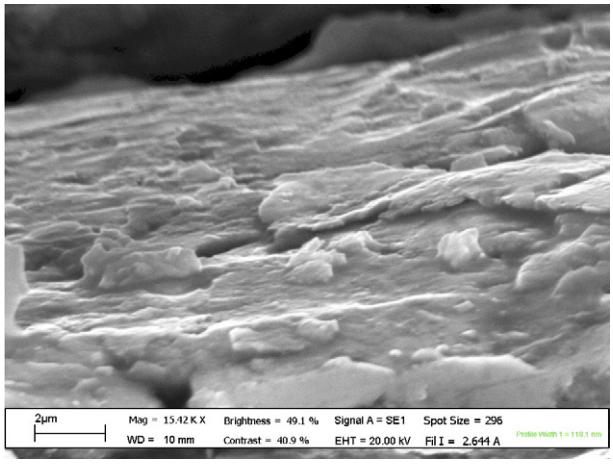

Fig. 2. SEM micrograph of VC film on Ti substrate.

effect was taken into account [17,18]. The reasonable expression for the H_c in this case is

$$H_c = H_{s0} + [B_s + 2ct(H_{f0} - H_{s0})]/D \quad (2)$$

where $c \cong 0.5$ for brittle hard film on a more ductile substrate [16]; H_{s0} and H_{f0} are intrinsic hardness of substrate and film, respectively; t is the film thickness; D is the imprint diagonal, and B_s is the coefficient, which can be determined from a separate experiment on the substrate hardness. To calculate the intrinsic hardness of the film, special attention was paid to correctly choose the indentation depths range, d, inside which the model is adequate. According to the estimations, the d/t ratio must be from about 2 to approximately 20 providing substrate-dominated mixed region where the film is fractured through-thickness as it is bent to conform to the plastically deformed substrate [19]. Over this range of d/t, the estimations based on the Jönsson and Hogmark model have been demonstrated to produce the best fit to the experimental hardness data and to coincide well with the estimations resulting from more complicated models [19,20]. In our case the relative penetration depth was from 6 to approximately 20 ($d = D/7$ for Vickers pyramidal indenter), otherwise all the data obtained from imprints with higher d/t were deleted from the sample data set. To evaluate H_{s0} and B_s values, experiments with the titanium substrate were performed. The experimental plot hardness of the substrate, H_s, *versus* the inverse of imprint diagonal, $1/D$, was well fitted by a linear regression, which provided values of 1.84 GPa and 5.38×10^{-6} GPa m, for H_{s0} and B_s, respectively. The Vickers microhardness approach was preferred because of the difficulty to obtain reproducible and reliable nanoindentation data for the rough film.

3. Results and discussion

SEM micrographs of films are shown in Figs. 2 and 3. The films are rough, partly due to the roughness of the sandblasted surface of the substrate, and partly to their layered morphology. Droplets of 0.2 to 2 μm size, originated from the expulsion of the target, are present on the film surface. The slit-like pores can be seen at the boundaries of the layers (Fig. 2). As estimated by SEM cross-sectional observation, thickness of all the films is ranging from 160 to 250 nm, approximately. This rough estimation due to the morphology of the surface correlates well with the microbalance data. According to the EDS data, the Me/C atomic ratio in the films is close to its stoichiometric ratio of 1:1.

Figs. 4 and 5 show the angular-dispersive XRD patterns for the substrate-film systems recorded by the Philips X'Pert PRO diffractometer. The peaks are broadened, indicating an ultrafine microstructure of the film, and shifted towards the long-wave region. The apparently ultrafine grains of the film are constituents of a rather coarse grained microstructure of the coating, as visible in Fig. 2. The reflection (111) of NbC with high expected intensity (according to JCPDS cards) becomes of low intensity, probably due to the textured microstructure of the coating (preferable orientation is (200)). It was difficult to conclude about the texture of the VC film due to overlapping of the VC (111) reflection with the high-intensity Ti (002) peak located at $2\theta = 38.45°$.

Peaks at $2\theta = 44.31°$ and 64.27° (Fig. 4(a)) can be attributed to the VC (200) and (220) reflections of the film deposited at 350 °C. An increase of substrate preheating temperature to 500 °C results in shifting of the peaks position to 43.91° and 63.83° (Fig. 4(b)). Respective reference peaks are located at 43.42° and 63.08°, according to the JCPDS card #73-0476. For the NbC film deposited at 350 °C, the peaks (200) and (220) are located at 41.85° and 60.57° (Fig. 5(a)), respectively. As the substrate temperature rises to 500 °C, the peaks position is shifting towards 41.07° and 59.17° (Fig. 5(b)). Respective NbC reference peaks are positioned at 40.32° and 58.34°. The shifting can be attributed to the residual stress imposed to the film. There may exist compressive thermal stresses, $\sigma = E_f(\alpha_f - \alpha_s)\Delta T$, imposed to the films owing to the cooling of the coated system in the deposition chamber, because the thermal expansion coefficients of carbides (α_f equals to 7.25×10^{-6} °C^{-1} for VC and 7.21×10^{-6} °C^{-1} for NbC [21]) are lower than that of titanium (α_s equals to 9.6×10^{-6} °C^{-1} [22]). A rough estimation results in compressive stress of approximately −330 MPa for VC ($\Delta T = 330$ °C) and −370 MPa for NbC ($\Delta T = 330$ °C), taking into account the Young modulus of the films, E_f, is 430 and 470 GPa for VC and NbC,

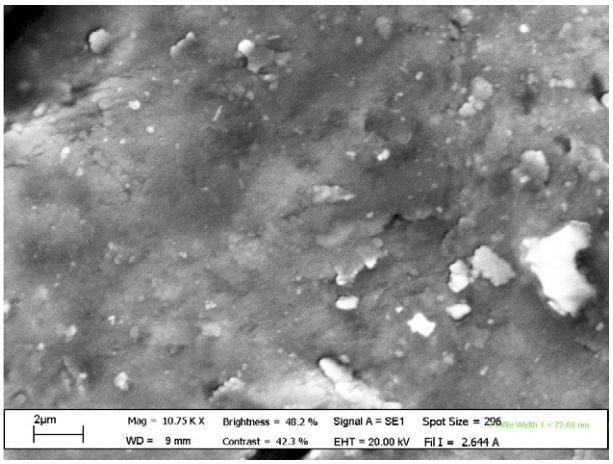

Fig. 3. SEM micrograph of NbC film on Ti substrate.

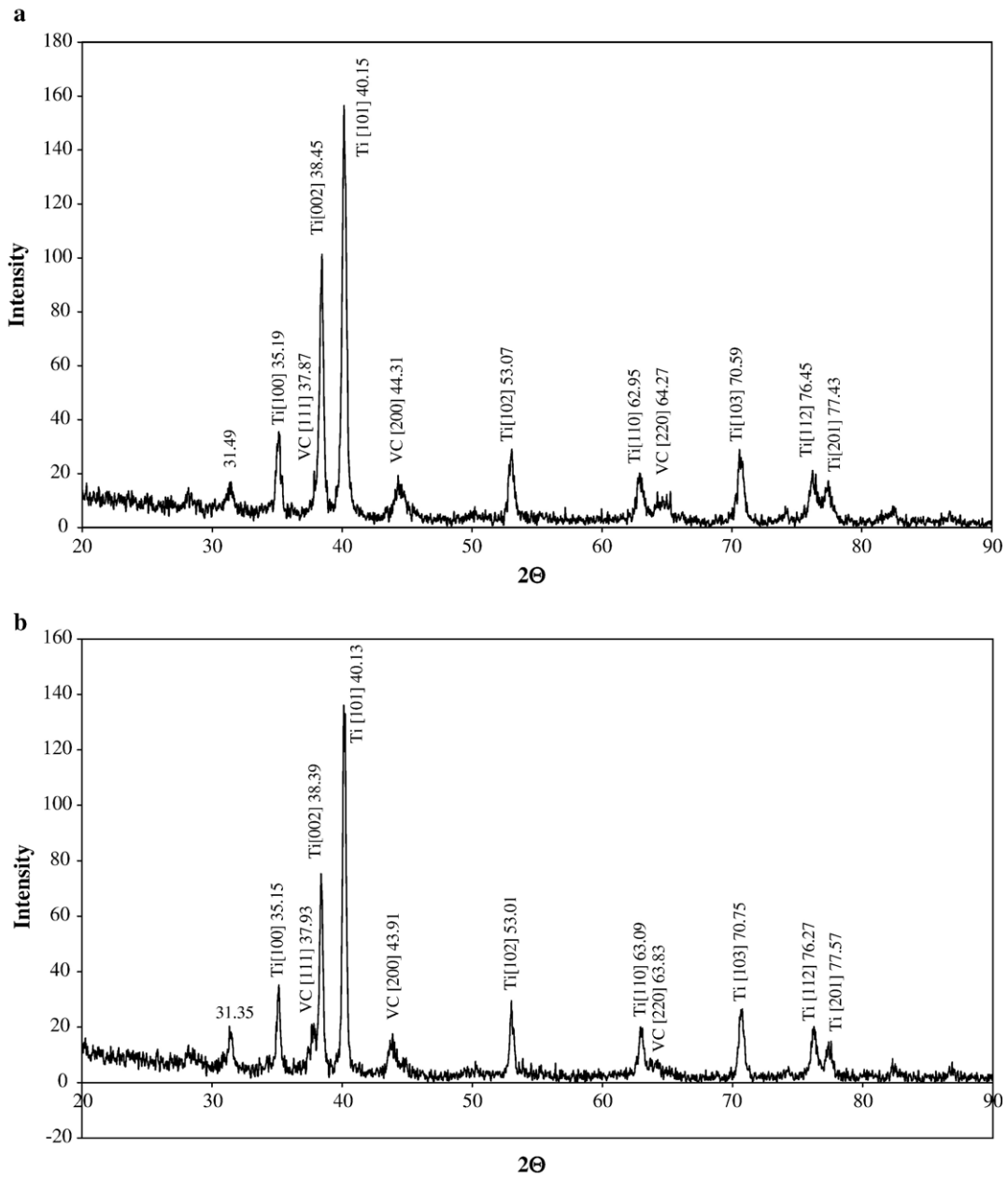

Fig. 4. X-ray diffraction pattern of: (a) VC film on Ti substrate (350 °C); (b) VC film on Ti substrate (500 °C).

respectively [1]. The VC and NbC films have smaller lattice constants than those for the standard powder sample (according to the JCPDS data). In the XRD measurements, the plane spacing, the grazing angle, and the wavelength of X-ray comply with the Bragg's equation. The peak shift towards small angle in the XRD spectra indicates the stress relaxation in the films deposited at 500 °C compared to those deposited at 350 °C. It could therefore be concluded that the substrate heating results in the compressive stress imposed to the films due to thermal expansion mismatch, but the heating at 500 °C allowed the thermal stress be partially relaxed, probably due to the recovery process.

Shown in Fig. 6 is the EDXD pattern for the Ti substrate coated by VC at the substrate preheating temperatures of 350 and 500 °C. The VC (200) reflection (q=2.95 (5) Å) is detectable for both films, regardless the substrate temperature, and a weak signal arising from the (220) orientation can be perceived too (circle in Fig. 6).

The rocking curve analysis was performed for both films in order to evaluate the film epitaxy by studying the Bragg reflections behaviour as a function of the asymmetry parameter defined in the Experimental section, in the ($-6°<\alpha<6°$) angular range. The measurement was performed by progressively tilting the sample (placed in the reflection geometry) at steps of 0.1° and collecting a diffraction pattern at each α-value. In the inset of Fig. 6, the rocking curve datapoints are shown for the VC/Ti system (deposition at 500 °C). The relative intensities deduced by the Gaussian fitting of the (200) reflection are randomly distributed, suggesting the crystallites to be randomly

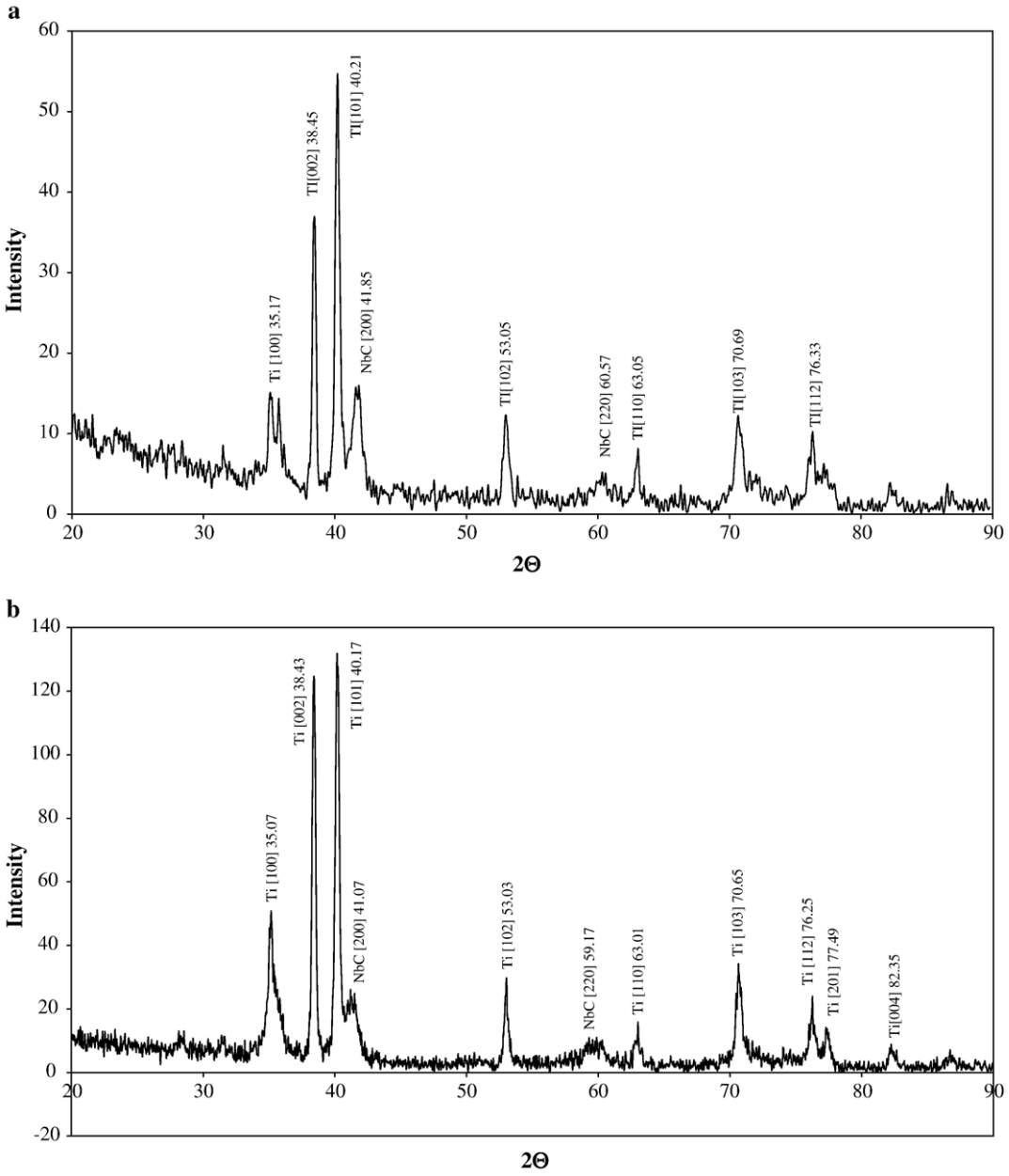

Fig. 5. X-ray diffraction pattern of: (a) NbC film on Ti substrate (350 °C); (b) NbC film on Ti substrate (500 °C).

rotated around their growth axes, with no correlation among adjacent domains. For the 350 °C film, no data processing could be performed, since the relative intensities associated with the (200) reflection were too weak.

NbC/Ti films (deposition temperatures 350 and 500 °C) were characterized by EDXD under the same experimental conditions described above for the VC films. Diffraction patterns were collected at $\vartheta = 6.2°$ in reflection mode and the experimental working conditions were kept unchanged during all the acquisitions. In Fig. 7, both the diffraction patterns are shown. As enhanced by the vertical arrow, the NbC (200) reflection ($q = 2.91(5)$ Å) is present in both samples and is partially convolved with the Ti (101) reflection. Moreover, the circle in Fig. 7 evidences the diffracted region around $q = 4$ Å where a weak contribution attributed to the NbC (220) peak can be detected. However, the intensity of this reflection can be neglected if compared to that of the (200) peak and it was possible to observe this contribution only due to the very high counting time (24 h) of these diffraction patterns. Strong fluorescence lines are also visible, being the Nb K_a and K_β at $E = 16.61$ KeV and $E = 18.62$ KeV.

The rocking curve data processing was possible only for the sample deposited at 350 °C, since the NbC (200) reflection detected from the 500 °C film is less intense than the signal arising from the previous film. In the inset of Fig. 7, the statistical distributions of the relative intensities deduced by the Gaussian fitting of the NbC (350 °C) (200) peak is shown, as a function of the asymmetry parameter. The intensities datapoints

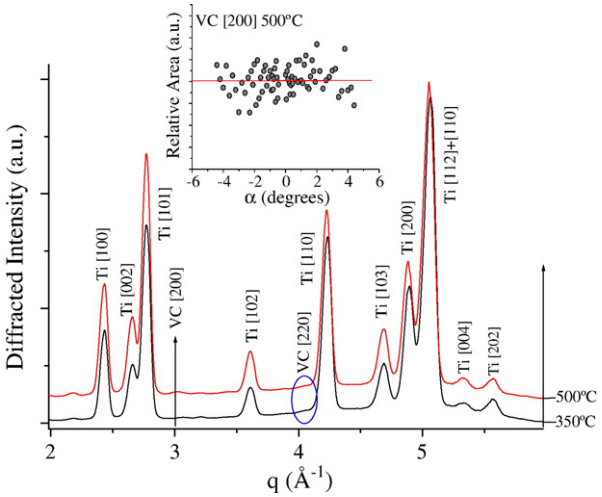

Fig. 6. ED diffraction patterns of VC/Ti films deposited at 350 °C (lower curve) and 500 °C (upper curve), collected as a function of the scattering parameter q. The preferred VC (200) Bragg reflection is scarcely visible at 350 °C and becomes more intense at 500 °C. The RC analysis of the latter reflection is shown in the inset.

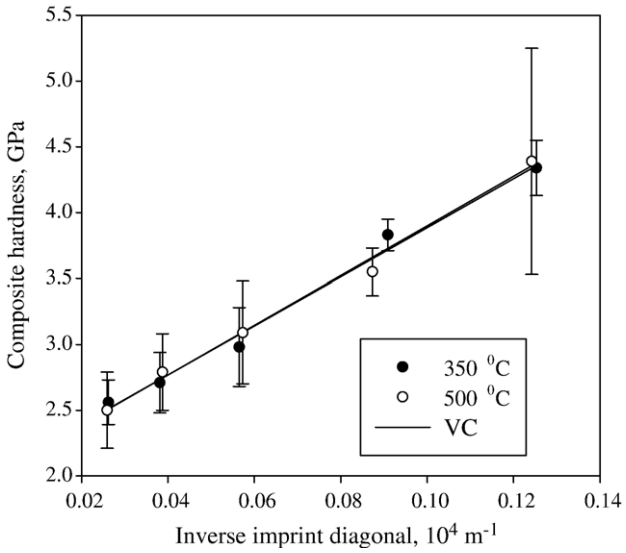

Fig. 8. Composite hardness of the VC film/Ti substrate system *versus* inverse imprint diagonal.

are randomly distributed around a mean value. This indicates the adjacent (200) crystallites of the NbC film to be distributed randomly, as in the case of vanadium carbide.

Figs. 8 and 9 show the composite hardness *versus* the inverse imprint diagonal plots. The plots are approximated well by a linear regression. A least squares fit of the lines to the Eq. (2) results in the slope $B_c=[B_s+2ct(H_{f0}-H_{s0})]$. Using the B_s and H_{s0} evaluated for the Ti substrate, the intrinsic hardness, H_{f0}, of the films was calculated. The results are given in Table 1 and compared to the literature data [1] on the hardness of VC and NbC bulk ceramics. The data for the films and the ceramics are in good agreement. With the increase in the substrate preheating temperature from 350 to 500 °C, the hardness of the VC and NbC films becomes somewhat lower, probably due to recovery process leading to a decrease in compressive stress level. This stress might hinder the indenter penetration increasing the measured hardness value. A strong correlation between the compressive stress and hardness has been observed for the thin NbN and NbC films deposited on silicon by a filtered vacuum cathodic arc deposition [23]. Compressive stress is associated usually with highly dense films [23,24]. Another factor effecting the hardness is microstructure and/or crystallographic quality of the film [25,26]. Particularly the layered morphology of the EB deposited VC and NbC films can be a factor diminishing the influence of the residual compressive stress on the measured hardness values.

Thus, it is possible to conclude that the EBD method allows the deposition of thin VC and NbC films on titanium, retaining intrinsic hardness of these refractory carbides, contrary to the

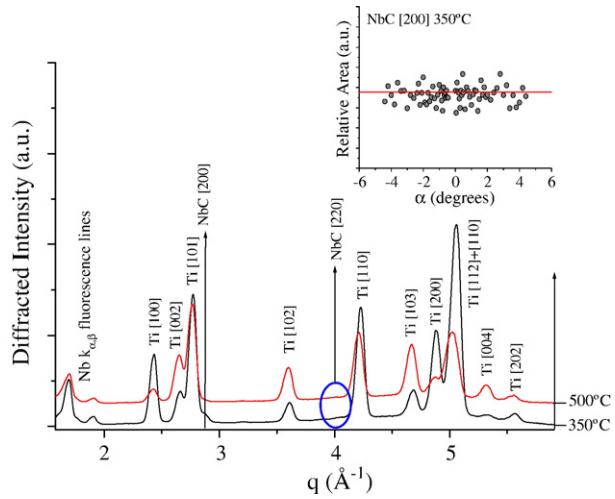

Fig. 7. ED diffraction patterns of NbC/Ti films deposited at 350 °C (lower curve) and 500 °C (upper curve), collected as a function of the scattering parameter q. The preferred NbC (200) Bragg reflection is visible at 350 °C, the rocking curve analysis of this peak being plotted in the inset.

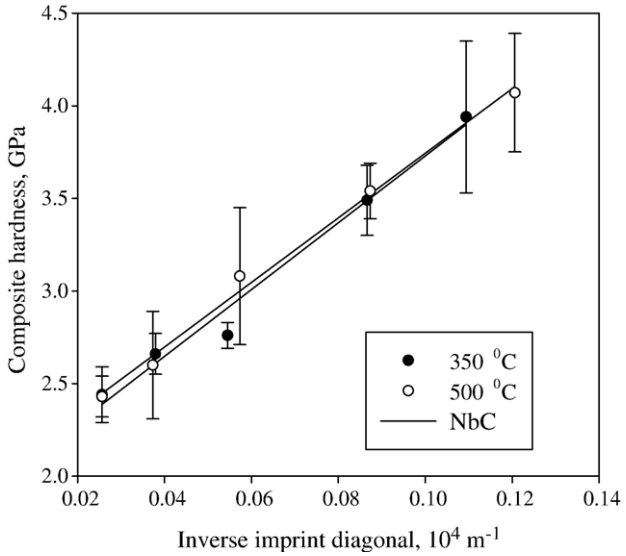

Fig. 9. Composite hardness of the NbC film/Ti substrate system *versus* inverse imprint diagonal.

Table 1
Hardness of electron beam deposited VC and NbC thin films on titanium substrate

Film/substrate system	Preheating substrate T, °C	Hardness, GPa	Hardness of bulk ceramics, GPa [1]
VC on Ti	350	25±1	20.2–26.5
VC on Ti	500	24±1	
NbC on Ti	350	21±1	15.0–21.9
NbC on Ti	500	18±1	

EB deposited TiC films. The hardness of the EBD TiC film on Ti substrate deposited under the same experimental conditions was revealed to decrease to 10–20 GPa compared to 30 GPa for bulk TiC, resulting from inter-diffusion of components from the film to the substrate [10]. There were no deviations from the stoichiometry revealed in the EBD VC and NbC films, according to the EDS data.

Further experiments are going to be performed to evaluate both tribological and *in vitro* biological behaviour of the coated systems under study to evaluate their possible application in orthopaedic devices.

4. Conclusions

Experiments were performed with the EB deposited VC and NbC thin films on sandblasted titanium substrate at different substrate preheating temperature (350 and 500 °C), and the intrinsic hardness of the films was separated from the measured composite hardness of the film–substrate system. The following conclusions can be drawn from the results of the present study:

1. EBD method allowed the fabrication of thin compact VC and NbC films on rough titanium substrate surface.
2. Both the EDXD rocking curve and the XRD (for NbC film) analyses revealed the films to have (200) preferred orientation and the films are supposed to be under the compressive stress.
3. The measured intrinsic hardness of the films is in good agreement with that of the respective bulk carbide ceramics.

Acknowledgment

The work is supported by the CNR-RAS project agreement.

References

[1] R.A. Andrievski, I.I. Spivak, Strength of Refractory Compounds and Related Materials, Metallurgy, Tcheljabinsk, 1989.
[2] A. Krajewski, L. D'Alessio, G. De Maria, Cryst. Res. Technol. 33 (1998) 341.
[3] J. Musil, Surf. Coat. Technol. 125 (2000) 322.
[4] S.C. Mishraa, B.B. Nayakb, B.C. Mohantyb, B. Millsc, J. Mater. Process. Technol. 132 (2003) 143.
[5] S. Barzilai, A. Raveh, N. Frage, Thin Solid Films 496 (2006) 450.
[6] M. Long, H.J. Rack, Biomaterials 19 (1998) 1621.
[7] C.O. Freeman, I.M. Brook, J. Mater. Sci. Mater. Med. 17 (2006) 465.
[8] A. Satoh, A. Kinbara, M. Kitagawa, H. Nanto, E. Kusano, Thin Solid Films 343/344 (1999) 254.
[9] M. Brama, N. Rhodes, J. Hunt, A. Ricci, R. Teghil, S. Miglaccio, C. Della Rocca, S. Leccisotti, A. Lioi, M. Scandurra, G. De Maria, D. Ferro, F. Pu, G. Panzini, L. Politi, R. Scandurra, Biomaterials 28 (2007) 595.
[10] D. Ferro, R. Scandurra, A. Latini, J.V. Rau, S.M. Barinov, J. Mater. Sci. 39 (2004) 329.
[11] U. Sen, Thin Solid Films 483 (2005) 152.
[12] D. Ferro, S.M. Barinov, J.V. Rau, A. Latini, R. Scandurra, B. Brunetti, Surf. Coat. Technol. 200 (2006) 4701.
[13] A. Latini, S.M. Barinov, D. Ferro, J.V. Rau, R. Scandurra, Powder Metall. Prog. 6 (2006) 20.
[14] R. Caminiti, V. Rossi Albertini, Int. Rev. Phys. Chem. 18 (1999) 263.
[15] B. Paci, A. Generosi, V. Rossi Albertini, E. Agostinelli, G. Varvaro, D. Fiorani, Chem. Mater. 16 (2004) 292.
[16] B. Jönsson, S. Hogmark, Thin Solid Films 114 (1984) 257.
[17] H. Bueckle, in: J.H. Westbrook, H. Conrad (Eds.), Science of Hardness Testing and Its Research Application, ASM Publ., Metals Park, 1973.
[18] A. Iost, R. Bigot, Surf. Coat. Technol. 80 (1996) 117.
[19] A.M. Korsunsky, M.R. McGurk, S.J. Bull, T.F. Page, Surf. Coat. Technol. 99 (1998) 171.
[20] E.S. Puchi-Cabrera, Surf. Coat. Technol. 160 (2002) 177.
[21] G.V. Samsonov, I.M. Vititskij, Refractory Compounds, Metallurgy, Moscow, 1976.
[22] C.I. Smithells, Metals Reference Book, Butterworth and Co. (Publishers) Ltd., London, 1976.
[23] A. Bendavid, P.J. Martin, T.J. Kinder, E.W. Preston, Surf. Coat. Technol. 163–164 (2003) 347.
[24] S.J. Bull, Vacuum 43 (1992) 387.
[25] J.A. Thornton, D.W. Hoffman, Thin Solid Films 171 (1989) 5.
[26] Z. Bi, R. Zhang, X. Wang, S. Gu, B. Shen, Y. Shi, Z. Liu, Y. Zheng, J. Am. Ceram. Soc. 86 (2003) 2059.